

THE EFFECTS OF STRESS PULSE CHARACTERISTICS ON THE DEFEAT OF ARMOUR PIERCING PROJECTILES

I. M. Pickup¹, A. K. Barker¹, B. J. James¹, C. Cottenot² and H. Orsini²

¹ DERA, Chobham Lane, Chertsey, Surrey KT16 OEE, England

² CTA, 16 Bis, Avenue Prieur de la Côte D'Or, 94114 Arcueil CEDEX, France

A study is in progress which seeks to decouple the interaction between the projectile and the composite transparent armour into constituent parts:

- parameters which induce damage to the penetrator
- the effect of penetrator damage on subsequent penetration
- mechanisms which confer penetration resistance to the absorbers.

This paper reports aspects of the first stage of the programme, which characterises the damage induced in the projectile (7.62 mm Armour Piercing, AP) as a function of: target impedance, impact stress pulse length, impact velocity and target geometry.

Target materials have been chosen to simulate a range of impedance (Z) from 15 to 38 MPa m⁻¹ s to represent those applicable to more traditional transparent armour materials and high performance variants being developed.

Significant differences in fracture morphology were observed. The effects of varying impedance, impact stress pulse and target geometry are discussed.

INTRODUCTION

Increased performance of transparent armour is required for lightweight armour protection for vehicles and helicopters. Traditional armour configurations entail a front glass layer (often laminated soda-lime glass), backed by a polymer layer which absorbs the energy from the projectile and failed glass by plastic deformation. A method being addressed for improving the performance of such armour is the introduction of non-traditional materials into composite lamellae [1,2]. High mechanical impedance materials such as polycrystalline glass ceramics, sapphire, and magnesium aluminate spinels are being introduced into the composite array to induce damage to the projectile. A fractured projectile is much easier to arrest than a projectile penetrating in a rigid body mode. Construction options may include layers of two or three material types. They may also include laminations within a layer type. Ballard [2] defined a three layer armour with transparent ceramic/glass/polycarbonate to defeat a 7.62 mm AP projectile. The front layer of high impedance material to initiate damage in the projectile, a second layer of glass to slow

and possibly further damage the projectile and the polymer layer to arrest all the damaged particles.

This paper is focussed primarily on aspects of damage induction in hard steel 7.62 mm armour piercing projectiles during impact on high impedance materials. In particular the resulting damage morphology and terminal ballistic effects resulting from changes in impedance, stress pulse length and lamination configurations have been studied. Opaque analogue materials have been used to simulate high impedance, and high cost, transparent materials such as aluminium oxynitride [3] or magnesium aluminate spinel [1].

This work forms the first part of a larger programme which considers, in addition to the penetrator damage analysis, the effect of initial damage on subsequent arrest in standard glass layers, the intrinsic energy absorption characteristics of the transparent armour and the mechanisms of arrest of the damaged material by the polymer backing layer. These aspects will be reported elsewhere.

Sintox FA alumina (SFA) (95%) manufactured by Morgan Matroc, UK has been used to simulate sapphire and aluminium oxynitride. The glass absorbers used were Soda-lime glass (SG) and an opaque lithia crystalline ceramic (identified as LZ1) to simulate the transparent ceramic with similar composition. Table 1 lists the key properties of materials used in the programme.

Table 1: Materials data

Material	Density ρ (kgm^{-3})	Impedance Z ($\text{MPa m}^{-1}\text{s}$)	Hardness (Hv)	Young's Mod, E (GPa)	Shear Mod G (GPa)
Sintox FA (SFA)	3694	36.5	1100	308	124
Soda-lime glass (SG)	2510	14.7	540	74	30
Glass ceramic (LZ1)	2334	15.5	-	95	40
Polycarbonate (PC)	1180	3.2	-	6	2

EXPERIMENTAL SETUP

The 7.62 N PPI Armour Piercing (AP) hard steel Athena round was chosen as the standard projectile. The core, which is partially brass jacketed (Fig. 1), is of high hardness steel $\sim 830 \text{ Hv}_{30}$ and has a weight of 5.8 g. A full service charge yielded a mean impact velocity of $826 \pm 3 \text{ ms}^{-1}$ with a muzzle to target distance of approximately 12 m.

The round was fired from a 7.62 mm Browning proof barrel. Velocity was measured using light screens set at 4 m before impact, and adjusted for retardation to calculate the impact velocity. The glass and ceramic targets had a ground, flat finish and were simply clamped together. Flash X-ray was used to measure the residual velocity of the projectile, and the physical condition immediately after perforation of the target. The projectile and the debris were soft recovered in sand to allow the characterisation of projectile damage, which included measurement of the projectile core mass remaining intact.

DAMAGE MORPHOLOGY

Standard low impedance glasses, such as soda-lime glass usually impart little damage to hard steel AP rounds. The projectiles tend to pass through in a relatively undeformed state. The glass absorbs kinetic energy simply by increasing drag on the projectile. The role of the high impedance materials is to induce damage, breaking the round, possibly with some erosion on the front surface before penetration [4], spreading the load to decrease the local pressure on the absorber.

We initially studied the effects of front face impedance and hardness on the morphology of penetrator damage by employing two types of high impedance material, silicon carbide ($Z=39.5 \text{ MPa m}^{-1}\text{s}$ and $H_v=2400$) and alumina SFA ($Z=36.5 \text{ MPa m}^{-1}\text{s}$ and $H_v=1100$). The impedance of each is similar but silicon carbide has considerably greater strength and hardness. The added value of extra hardness (in addition to the increased impedance) is not clear but may result in increased deviatoric strength and higher KE absorption. In practice, both silicon carbide and alumina produced similar, significant increases in damage compared to the lower Z glasses. This paper will therefore consider only the difference between high and low Z materials. The role of hardness in the high Z group will be dealt with elsewhere.

The captured rounds from shot 104, impacting a low impedance LZ1 (10 mm) target and shot 118 impacting a high impedance SFA (8 mm) are shown in Fig. 1. There is a very clear difference in fracture morphology. For LZ1 the tip is barely blunted compared to the blocky type fracture which has reduced the residual core mass to ~40% of the original value.

Both target interactions caused fracture across the diameter of the core suggesting spall or bending stresses.

A simple 1-D analysis based on the relative impedance of the targets and the steel round impacting at 850 ms^{-1} would indicate the impact stress induced in the steel core when impacting SFA would be greater than 40% higher than when impacting LZ1. In practice, the geometry of the impact, damage, and plasticity will alter this figure. However, the impact stress is considerably greater for the high impedance material. It would be desirable to determine experimentally the impedance value at which point there is a transition in the characteristic fracture morphology. Unfortunately, no materials were available with intermediate impedance which also have sufficiently high strength to impart intermediate impact stresses.

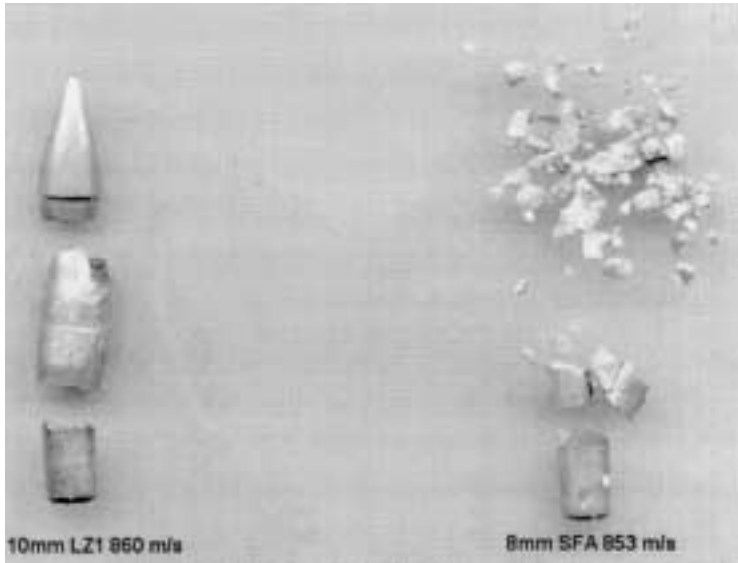


Figure 1: The effect of target impedance on round damage

We considered the mechanisms which may be controlling the characteristic damage morphology. Does the impact stress pulse cause incipient damage, as it travels down the projectile, which will be activated as it passes through the lower impedance glass absorber layer? If this is the case, how much of the high impedance layer is required to cause this impulse effect? Does the blocky fracture and erosion process occur only during passage through the high impedance layer? We carried out a parametric study in which the relative levels of stress pulse magnitude and duration were varied.

PARAMETRIC STUDY

A series of impact tests were performed in which the impact stress pulse was varied by using a high impedance (Z) front layer ranging from 0 to 6 mm with lower impedance absorbing layers of different thickness and material. These layers were backed with 9 mm of polycarbonate. The velocity ratio, R , (residual velocity, V_R / impact velocity, V_i) has been plotted as a function of high impedance layer thickness for the various absorbing layers.

Figure 2 clearly shows the efficacy of high Z front layers. For targets without a high Z layer, the velocity ratio reduced from 0.98 to 0.82 when the soda glass thickness was increased more than threefold from 8 mm to 25.4 mm. Assuming a linear reduction in velocity ratio with thickness, the decrement rate, $dR/dt = -0.009 \text{ mm}^{-1}$. When the high impedance SFA layer was used, the same decrement that took a threefold increase in SG thickness was achieved by adding only 2 mm of SFA. Assuming a linear reduction in velocity ratio with thickness over the 6 mm experimental range, the decrement rate $dR/dt = -0.16 \text{ mm}^{-1}$.

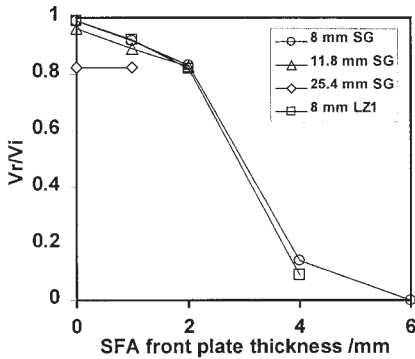


Figure 2: The effect of high impedance layer (SFA) thickness on velocity ratio (R) for various absorber configurations.

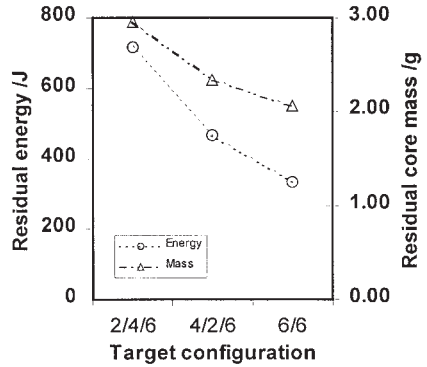


Figure 3: Partitioned front high z layer experiments at constant path length and impact velocity. The last number refers to the 6 mm SG backing, the preceding number(s) refer to the thickness in mm of the SFA layer(s).

The areal density for defeat of the 7.62 mm Athena AP round for the configuration 6 mm SFA/ 8 mm soda-glass/ 9 mm PC is 53 kg m^{-2} . This compares with an areal density of $>100 \text{ kg m}^{-2}$ for conventional systems containing only low Z layers. A system containing the aluminium oxynitride for which SFA is a simulant may even exceed this performance.

The LZ1 absorbing layer did not perform significantly differently to the SG.

Figure 2 shows a monotonically decreasing velocity ratio ($R = V_r/V_i$) as the high Z material thickness increases. There appears to be insufficient evidence here to support our initial hypothesis that a critical value of stress amplitude and stress duration is required to initiate fracture in the projectile. Although the length of the stress pulse imparted to the projectile changes with the thickness of the front, high Z layer, so does the total thickness of high Z material. In order to decouple the effects of stress pulse length and thickness of high Z layer, a further investigation was undertaken.

IMPACT PULSE LENGTH

In order to measure the effects of changing the impact induced stress pulse length independently of the thickness of the high Z front layer, we used different layered configurations of the same total thickness. Three configurations were used:

- i) 2 mm SFA / 4 mm SFA / 6 mm SG
- ii) 4 mm SFA / 2 mm SFA / 6 mm SG
- iii) 6 mm SFA / 6 mm SG.

Separation of the front high Z layers was effected using a $40 \mu\text{m}$ polyethylene layer. This ensured an effective impedance interface between the 2 mm layer and the 4 mm layer, and resulted in the initiation of stress pulses of different duration. Assuming a lon-

gitudinal wave speed of $\sim 10 \text{ km s}^{-1}$ this would equate to impact pulse lengths of 0.4, 0.8 and $1.2 \mu\text{s}$ respectively. The impact velocity was constant at 826 ms^{-1} .

The different partitioning configurations had a significant effect on the damage induced in the projectile. This is seen in Figure 3 as reducing residual energy as the front SFA layer increased from 2 to 6 mm (with the total SFA thickness remaining constant). The monolithic, 6 mm front block of SFA resulted in a penetrator residual energy less than half that for a 2 mm front block (333 J compared with 716 J). This reduction in residual energy was due to both a reduction in penetrating core mass and a reduction in residual velocity.

To aid understanding of the effect of the layering on the stress pulse formation in the projectile a simplified problem was simulated numerically using the Lagrange code AUTODYN in a 2-D mode. The problem was set up as a 100 mm long, 6 mm diameter rod impacting targets of the same partitioned configuration (2/4, 4/2 and 6 mm) as described above for the front, high Z layer. In this case the backing of SG was omitted. The output, Fig. 4 is the principal stress history in the axis direction of the rod at a position 25 mm from the impact surface. The rod was treated as a perfectly elastic solid and the SFA was modelled using a Johnson-Holmquist-2 (JH2) [5] ceramic model calibrated for SFA. A polymer model was used for the impedance break material.

Although the rod was modelled with flat ends, the calculated stress pulse rise time is quite slow, $\sim 1.5 \mu\text{s}$. This is a significant time when considering the range of theoretical pulse lengths is 0.4 to $1.2 \mu\text{s}$. However, slight increments in pulse length are determined as the front layer thickness increases. More significant, however, is the increase in the magnitude of the stress pulse as the front layer thickness is increased.

The decrease in stress pulse magnitude with decreasing front face thickness (total thickness of high Z front face remaining constant) is due to earlier initiation of damage to the layer by earlier reflection of a release wave at the impedance discontinuity. This reduces the strength and the effective dynamic impedance of the target material. As the front layer increases in thickness, the time for the damage front to return from the back surface increases and a relatively higher proportion of the material ahead of the penetrator is still compressed and consequently strong. This effect has also been observed in thicker laminated targets [6].

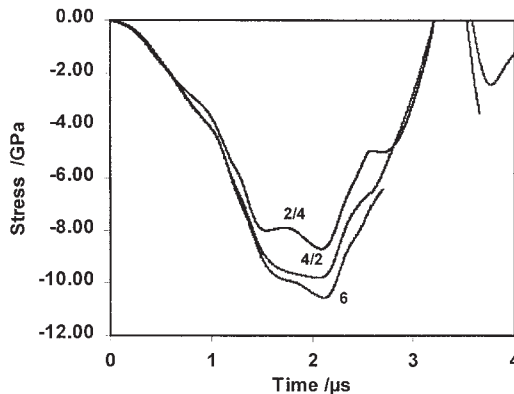


Figure 5: Numerical simulation of the stress pulse history in the schematic rod, impacting the partitioned SFA targets at a velocity of 860 m/s.

The increased performance of the thicker front layer seems therefore to be due to increased stress amplitude in the penetrator and not to increased stress duration, as originally surmised.

CONCLUSIONS

A parametric study has been performed investigating the damage morphology of hard steel 7.62 mm AP projectiles through impact on simulants of transparent armour systems. The effects of target impedance, hardness and geometry were studied.

The degree of damage to the AP round and the morphology of this damage is primarily influenced by the dynamic deviatoric strength of the target layers. When a threshold target hardness is exceeded damage is initiated in the penetrator immediately adjacent to the target interface. This leads to fracture and erosion.

The effect of the characteristics of the impact stress pulse initiated in the projectile has been assessed by experiment and numerical simulation. The effects of pulse shape were found to be minimal.

The effective dynamic deviatoric strength of ceramic/glass layers is dependent on layer thickness. This is due to damage originating from the back surface of the layer, releasing constraining pressure. This release occurring earlier for thinner layers.

Triple layered systems including a high impedance front layer, a low impedance glass absorber layer and a polymer backing layer have been investigated. A systematic study of simulant systems indicates that areal densities of practical, transparent armours may be reduced to 50% the value of traditional low impedance glass systems, by the incorporation of relatively thin high impedance front face layers.

ACKNOWLEDGEMENTS

The authors are grateful to Ed Rothead and Jenny Penwarne of DERA, Chertsey, for their enthusiastic assistance in the numerical simulation.

The work reported in this paper was performed within a UK/French collaborative defence research programme.

REFERENCES

1. Cottenot C. E., Transparent ceramic for light weight armours, Lightweight Armour Symposium 95, Cranfield, England, 28–30 June, 1995
2. Ballard C. P., Transparent ceramic armour, Sandia Laboratories report, SAND77-1736, May, 1978.
3. Maguire E.A., Rawson J.K. and Tustison R. W., Aluminium oxynitride's resistance to impact and erosion, Published in Window and Dome Technologies IV, Ed. P. Klocek, SPIE Proceedings 2286, pp. 26–32, 1994.
4. Gooch W. A., Burkins M. S., Kingman P., Hauver G., Netherwood P., and Benk R., Dynamic X-ray imaging of 7.62 mm APM2 projectiles penetrating boron carbide, 18th International Symposium on Ballistics, San Antonio, TX, 15–19 Nov., 1999
5. Johnson G. R. and Holmquist T. J., An improved computational constitutive model for brittle materials, High Pressure Science and Technology, AIP, New York, pp. 981–984, 1994.
6. Richards M., Clegg R. and Howlett S., Ballistic performance assessment of glass laminates through experimental and numerical investigation, 18th International Symposium on Ballistics, San Antonio, TX, 15–19 Nov., 1999

© Crown Copyright 2001 Published with the permission of the Defence Evaluation and Research Agency on behalf of the Controller of HMSO